Wireless Pers Commun (2014) 77:1751–1773
DOI 10.1007/s11277-014-1607-4

Performance Analysis of Amplify-and-Forward Relay Systems with Interference-Limited Destination in Various Rician Fading Channels

Anas M. Salhab · Fawaz S. Al-Qahtani · Salam A. Zummo · Hussein Alnuweiri

Published online: 24 January 2014

Abstract In this paper, we investigate the performance of a dual-hop fixed-gain amplify-and-forward relay system in the presence of co-channel interference at the destination node. Different fading scenarios for the desired user and interferers' channels are assumed in this study. We consider the Rician/Nakagami-*m*, the Rician/Rician, and the Nakagami-*m*/Rician fading environments. In our analysis, we derive accurate approximations for the outage probability and symbol error probability (SEP) of the considered scenarios. The generic independent non-identically distributed (i.n.d.) case of interferers' channels is considered for the Rician/Nakagami-*m* scenario; whereas, the independent identically distributed (i.i.d.) case is studied for the Rician/Rician and the Nakagami-*m*/Rician environments. Furthermore, to get more insights on the considered systems, high signal-to-noise ratio (SNR) asymptotic analysis of the outage probability and SEP is derived for special cases of the considered fading scenarios. Monte-Carlo simulations and numerical examples are presented in order to validate the analytical and asymptotic results and to illustrate the effect of interference and other system parameters on the system performance. Results show that the different fading models of interferers' channels have the same diversity order and that the interference degrades the system performance by only reducing the coding gain. Furthermore, findings show that the case where the fading parameter of the desired user first hop channel is better than that of the second hop gives better performance compared to the vise versa case, especially, at low SNR values; whereas, both cases almost behave the same at high SNR values where the

A. M. Salhab (✉) · S. A. Zummo
Department of Electrical Engineering, King Fahd University of Petroleum and Minerals, Dhahran 31261, Saudi Arabia
e-mail: salhab@kfupm.edu.sa

S. A. Zummo
e-mail: zummo@kfupm.edu.sa

F. S. Al-Qahtani · H. Alnuweiri
Electrical and Computer Engineering Program, Texas A&M University at Qatar, Doha, Qatar
e-mail: fawaz.al-qahtani@qatar.tamu.edu

H. Alnuweiri
e-mail: hussein.alnuweiri@qatar.tamu.edu

performance of the system is dominated by the interference affecting the worst link. Finally, results show the big gap in system performance due to approximating the Rician fading distribution with the Nakagami-*m* distribution which is an indication on the inaccuracy of making such approximations in systems like the considered.

Keywords Relay networks · Amplify-and-forward · Co-channel interference · Rician fading · Nakagami-*m* fading

1 Introduction

Cooperative or relay networks have generally been studied with respect to the relay selection schemes, coding, multi-user communication, multi-antenna and beamforming, channel estimation errors, and power allocation, mostly, under conditions of additive white Gaussian noise (AWGN) [1–3]. However, the co-channel interference (CCI) dominates AWGN in such wireless systems due to the extensive re-use of frequency bands by system users. Moreover, the effect of CCI can be more severe on the relay systems where all relays may use the same frequency band and hence, CCI may exist in every link in the relay network. In [1], Laneman et al. introduced several relaying schemes among which are the amplify-and-forward (AF) and the decode-and-forward (DF). In AF, the relay simply amplifies the source signal and re-sends it again to the destination; whereas, in DF, some signal processing needs to be performed by the relay before the signal being forwarded. In general, the AF systems are classified into two subcategories, the channel-state information (CSI)-assisted gain relays, which use the instantaneous CSI from the previous hop, and the fixed-gain relays, which introduce a fixed gain in forwarding the source signals. The CSI-assisted AF relay systems require continuous estimation of the fading channel in order to produce their gain and to limit the relay output power. In contrast, fixed-gain relay systems introduce a fixed scale to the received signal regardless of the fading amplitudes which leads to a variable signal power at the relay output. Obviously, fixed-gain relays have a lower complexity compared to CSI-assisted relays. Despite of the inherent effect of interference in wireless systems, most of the conducted research on the AF and DF relay systems assume noise-limited environments; whereas, few papers study this effect on the performance of such cooperative systems. In general, the interference effect on system performance can be considered at the relay, at the destination, or at both. A situation where the interference may exist only at the relay node is in the frequency-division relay systems where the relay and destination terminals experience different interference patterns [4]. In [4], an approximate expression for the outage probability of a DF relay system with arbitrary number of interferers was derived assuming Nakagami-*m* fading channels. In [5], Al-Qahtani et al. studied the impact of arbitrary number of interferers at the relay node on the performance of a CSI-assisted AF relay system where closed-form expressions for the outage probability and SEP were derived assuming Nakagami-*m* fading channels. Furthermore, the authors evaluated those measures at the high SNR regime. In [6], a closed-from expression for the outage probability and an approximate expression for the bit error probability were derived for a CSI-assisted AF relay system assuming Nakagami-*m* fading channels and an interferer at the relay. The assumption of Rayleigh or Nakagami-*m* fading in such systems may not be accurate for situations where line-of-sight (LOS) components exist between the interferers and the relay in the desired cell. Such a situation can be seen in pico-cell relay systems where the interferers channels are Rician distributed [17]. In relay systems, considering the interference at the destination node is particularly relevant to time-division multiple-access (TDMA) systems in which a single time-slot is shared by many

relays [7]. This greatly motivates the model where a destination is corrupted by many interferers. In [8], the authors evaluated closed-form expressions for both the outage and asymptotic outage probability of fixed-gain AF and DF relay systems in Rayleigh fading environments. A key result of this study is that the worst behavior happens when the interference power is equally distributed between the interferers. In [9], exact expressions for both the outage and asymptotic outage probability and SEP were derived with all links assumed to follow the Nakagami-m distribution. Again, in situations where LOS components exist between the interferers and the desired destination, the Rayleigh and Nakagami-m assumptions may not reflect the accurate behavior of the studied systems.

A more general scenario in relay networks is to consider the interference impact at both the relay and destination nodes. An early study that considered the interference at the relay and destination in relay systems was appeared in [10], in which the authors evaluated the performance of a dual-hop CSI-assisted AF relay system with an arbitrary number of interferers of i.i.d. fading channels. The outage probability was numerically evaluated assuming Nakagami-m fading channels. The outage probability of a fixed-gain AF relay system with interference at the relay and destination over Rayleigh and Nakagami-m fading channels was derived in closed-form expression in [11] and [12], respectively. In [13], the authors evaluated the outage performance of a CSI-assisted AF relay system when the desired user channels are Rician distributed and the interferers' channels follow the Rayleigh distribution. In [14], the authors derived both the outage probability and SEP of a CSI-assisted AF relay system over Rayleigh fading channels. They further evaluated the asymptotic outage probability and SEP assuming i.n.d. and i.i.d. interferers' fading channels. More on the interference at the relay and destination nodes in relay systems can be found in [15,16]. Again, the situation where LOS components may exist between the interferers and the desired relay and destination are not widely studied.

Despite of the importance of Rician fading, only few studies considered such a channel model in literature. It is known that the Rician distribution models wireless propagation comprising a LOS component in addition to other scattered components. The presence of LOS has been confirmed through physical measurement for a number of applications, such as micro-cellular mobile and indoor radio. LOS arises in ad-hoc network applications (especially for dense networks), which are currently receiving considerable interest. In such networks, due to the presence of a LOS propagation between the base station and users in the desired cell, it is acceptable to assume Rician fading for the desired user channels and Nakagami-m or Rayleigh fading for the interferers' channels. Another fading model that can be considered for interferers' channels is the Rician distribution as in micro-cell and pico-cell networks (radii in the range of 10–100 m) where the size cell is small as in buildings, markets, and industrial compounds [17]. We would like to note that approximating the Rician fading with other distributions such as the Nakagami-m as an example, may not give accurate results in some situations as will be shown in our findings. Also, it may not reflect the actual behavior of the system currently under consideration. Other important fading models that can be considered in relay networks is to assume Nakagami-m fading for the desired user channels and Rician fading for the interferers' channels. The importance of these models is that they are very general and accurately reflect the impact of the interference and other parameters on the behavior of studied systems. Such fading models were used in [18] in which Suraweera et al. considered two scenarios; noisy relay and destination with interference at the relay, and noisy relay with interference and an interference-limited destination. The desired user channels were assumed to be Rayleigh faded while the single interferer was assumed to follow Rician distribution. A key result of this study is that the overall system performance is hardly affected by the Rician-K factor of the interfering signal.

To the best of authors' knowledge, none of the literature studies considered the performance of fixed-gain AF relay systems with the desired user and interferers' channels being Rician/Nakagami-m, Rician/Rician, and Nakagami-m/Rician, respectively. As mentioned before, considering the interference at the destination node is particularly relevant to TDMA systems in which a single time-slot is shared by many relays. Furthermore, the assumption of Rician fading is motivated by the fact that it is used to model wireless propagation comprising a LOS component and a scattered component which is most likely to be existed in micro-cellular mobile and indoor radio. Also, the proposed fading models find their practicality in pico-cells as the dense ad-hoc networks. In our paper, we derive accurate approximations for the outage probability and SEP for the Rician/Nakagmi-m fading scenario for i.n.d. and i.i.d. interferers' channels. In addition, we derive accurate approximate expressions for the outage probability and SEP for both the Rician/Rician and the Nakagami-m/Rician fading scenarios for i.i.d. interferers' channels. The derived analytical expressions quantify the impact of interference on the performance of relay networks for a large set of fading environments. Further, the analysis of Rician channels is generally more difficult and as a special case, includes the commonly assumed Rayleigh fading. Finally, in order to get more about the system insights, we evaluate the asymptotic system performance at high SNR values for special cases of the proposed fading environments. The asymptotic outage probability and SEP in addition to the diversity order and coding gain are derived and compared.

This paper is organized as follows. Section 2 presents the system model. The outage, symbol error probability, and asymptotic performance of the proposed fading scenarios are respectively analyzed in Sects. 3, 4, and 5. Some simulation and numerical results are given and discussed in Sect. 6. Finally, conclusions are provided in Sect. 7.

2 System Model

Consider a dual-hop relay where a source node S transmits to a destination node D with the assistance of a relay node R. The entire communication takes place in two separate phases. In the first phase, S transmits the signal to R and then in the second phase the received signal at R is amplified with a gain and then forwarded to D. We consider that the signal at D is corrupted by interfering signals from N co-channel interferers $\{x_i\}_{i=1}^{N}$, each with an average power of P_i. The received signal at R can be expressed as

$$y_{\mathsf{r}} = h_{\mathsf{sr}} x_0 + n_{\mathsf{sr}}, \tag{1}$$

where h_{sr} is the channel coefficient for S-R link, x_0 is the transmitted symbol with $\mathbb{E}\{|x_0|^2\} = P_0, n_{\mathsf{sr}} \sim \mathcal{CN}(0, N_0)$ denotes the additive white Gaussian noise, and $\mathbb{E}\{\cdot\}$ denotes the expectation operation. In the second phase, the received signal at R is first scaled with the gain $\mathsf{G} \triangleq \sqrt{\frac{P_{\mathsf{r}}}{P_0\sigma_{\mathsf{sr}}^2+N_0}}$ and forwarded to D, where P_{r} is the power at R, and $\sigma_{\mathsf{sr}}^2 = \mathbb{E}\{|h_{\mathsf{sr}}|^2\}$. In practical situations where different time-slots are used by the source and a single time-slot is shared by many relays as in TDMA systems, the interference effect appears only at the destination node [7]. Therefore, the signal at D can be expressed as

$$y_{\mathsf{d}} = \mathsf{G} h_{\mathsf{rd}}(h_{\mathsf{sr}} x_0 + n_{\mathsf{sr}}) + \sum_{i=1}^{N} h_i x_i + n_{\mathsf{rd}}, \tag{2}$$

where h_{rd} denotes the channel coefficient for the R-D link, $\{h_i\}_{i=1}^{N}$ are the channel coefficients from interferers to D, and $n_{\mathsf{rd}} \sim \mathcal{CN}(0, N_0)$.

From (2), the end-to-end (e2e) signal-to-interference plus noise ratio (SINR) at D can be written as

$$\gamma_{\mathsf{D}} = \frac{\mathsf{G}^2 |h_{\mathsf{rd}}|^2 P_0 |h_{\mathsf{sr}}|^2}{\sum_{i=1}^{N} P_i |h_i|^2 + \mathsf{G}^2 N_0 |h_{\mathsf{rd}}|^2}. \tag{3}$$

As the destination is interference-limited, the effect of n_{rd} has been neglected in last result. This assumption is acceptable in practical situations where the interference is a crucial factor that governs the overall system performance as compared to noise [8].

Substituting G in (3), and after some algebraic manipulations, the e2e SINR can be written as $\gamma_{\mathsf{D}} = \frac{X_1 X_2}{CY + Y + X_2}$, where $X_1 = \frac{P_0}{N_0}|h_{\mathsf{sr}}|^2$, $X_2 = P_r |h_{\mathsf{rd}}|^2$, $C = \frac{P_0 \sigma_{\mathsf{sr}}^2}{N_0}$, and $Y = \sum_{i=1}^{N} Y_i$, where $Y_i = P_i |h_i|^2$.

In the rest of the paper, the system performance is analyzed for different fading environments, Rician/ Nakagami-m, Rician/Rician, and Nakagami-m/Rician.

3 Rician/Nakagami-m Environment

In this section, we evaluate the outage and symbol error probability performance of the Rician/Nakagami-m fading environment. Such fading scenario finds its applicability in micro-cellular mobile and indoor radio where a LOS propagation is existed between the base station and users in the desired cell.

3.1 Outage Probability

In this subsection, we derive the outage probability for the i.n.d. and i.i.d. cases of interferers' channels.

For this scenario, the channel coefficients of the desired user $h_{\mathsf{sr}}, h_{\mathsf{rd}}$ are Rician distributed, while the interferers' channels coefficients h_i are Nakagami-m distributed. Based on that, the channel gains $|h_{\mathsf{sr}}|^2, |h_{\mathsf{rd}}|^2$ are non-central chi square distributed with parameters K_1 and $\frac{1}{\eta_1}$, K_2 and $\frac{1}{\eta_2}$ respectively, and the gains $|h_i|^2, i = 1, \ldots, N$, are i.n.d. gamma distributed with parameters m_{I_i} and α_{I_i}.

Lemma 1 *The outage probability of the Rician/Nakagami-m fading scenario can be evaluated for the case of i.n.d. interferers' channels as*

$$P_{\text{out}}(\gamma_{\mathsf{th}}) = 1 - \exp\left(-\left(K_1 + K_2\right)\right) \exp\left(-\frac{1 + K_1}{\eta_1}\gamma_{\mathsf{th}}\right) \sum_{k=0}^{N} \Omega_{I_k}^{m_{I_k}} \sum_{i=1}^{m_{I_k}} \frac{\beta_k^{i-1}}{(i-1)!} \sum_{n=0}^{M_1} K_2^n \sum_{j=0}^{M_2} K_2^j$$

$$\times \frac{\Gamma(j + m_{I_k})}{j!\,\Gamma(n + j + 1)} \Xi_1^{\frac{j}{2}} \gamma_{\mathsf{th}}^{\frac{j}{2}} \sum_{l=0}^{M_3} \frac{K_1^l}{(l!)^2} \left(\frac{1 + K_1}{\eta_1}\right)^l \gamma_{\mathsf{th}}^l \sum_{q=0}^{l} \binom{l}{q} \Gamma(q + m_{I_k} + 1) \Xi_2^{\frac{q}{2}} \gamma_{\mathsf{th}}^{\frac{-q}{2}} \exp\left(\frac{\Xi_1}{2}\gamma_{\mathsf{th}}\right)$$

$$\times W_{a,b}\left(\Xi_1 \gamma_{\mathsf{th}}\right), \tag{4}$$

where γ_{th} *represents the outage threshold SNR,* $\beta_k^{i-1} = \frac{\prod_{l=1}^{N} \alpha_{I_l}^{m_{I_l}}}{(m_{I_k} - i)!} \frac{d^{i-1}}{ds^{i-1}} \left[\prod_{\substack{n=1 \\ n \neq k}}^{N} \left(\alpha_{I_n} + s\right)^{-m_{I_n}}\right]\Big|_{s=\alpha_{I_k}}$, $M_{(.)}$ *are parameters for series convergence and take values from 1 to 50,* $\Xi_1 = \Omega_{I_k}(1 + K_1)(1 + K_2)(C + 1)/\eta_1\eta_2$, $\Xi_2 = \eta_1 \Omega_{I_k}(1 + K_2)(C + 1)/\eta_2(1 + K_1)$ $W_{.,.}(\cdot)$ *is the Whittaker function defined in [19, Eq. (9.22)],* $a = -\left(\frac{j}{2} + \frac{q}{2} + m_{I_k}\right)$, *and* $b = \frac{-j+q+1}{2}$.

Proof To derive the outage probability for the i.n.d. case of the Rician/Nakagami-m fading scenario, the cumulative distribution function (CDF) of γ_{D}, conditioning on X_1 and Y, can be first expressed as

$$F_{\gamma_{\mathsf{D}}}(\gamma_{\mathsf{th}}) = \Pr\left(\frac{X_1 X_2}{CY + Y + X_2} \leq \gamma_{\mathsf{th}}\right) = \int_0^\infty \Pr\left(X_2 \leq \frac{\gamma_{\mathsf{th}}\,(y(C+1))}{w - \gamma_{\mathsf{th}}}\right) f_{X_1}(w) f_Y(y) dw dy, \tag{5}$$

where $\Pr(.)$ denotes probability, $f_{X_1}(w)$ and $f_Y(y)$ are the probability density function (PDFs) of X_1 and Y, respectively.

With change of variables, (5) can be rewritten as

$$F_{\gamma_{\mathsf{D}}}(\gamma_{\mathsf{th}}) = 1 - \int_0^\infty \Pr\left(X_2 \geq \frac{\gamma_{\mathsf{th}}(C+1)y}{z}\right) f_{X_1}(z + \gamma_{\mathsf{th}}) f_Y(y) dz dy. \tag{6}$$

To evaluate (6), the complement CDF of X_2, the PDF of X_1, and the PDF of Y are required, where X_1 and X_2 are non-central chi square distributed RVs with parameters K_1 and $\frac{N_0}{P_0 \eta_1}$, K_2 and $\frac{1}{P_r \eta_2}$ respectively, and Y is a summation of independent gamma distributed RVs with parameters m_{I_i} and α_{I_i}.

The CDF of X_2 and the PDF of X_1 are respectively given by

$$F_{X_2}(x) = 1 - Q\left(\sqrt{2K_2}, \sqrt{\tfrac{2(1+K_2)}{\eta_2} x}\right), \tag{7}$$

$$f_{X_1}(x) = \tfrac{1+K_1}{\eta_1} \exp\left(-K_1 - \tfrac{(1+K_1)}{\eta_1} x\right) I_0\left(2\sqrt{\tfrac{(1+K_1)K_1}{\eta_1} x}\right), \tag{8}$$

where $Q(.,.)$ is the Marcum Q-function and $I_0(.)$ is the Modified Bessel function of first kind and order zero defined in [19, Eq. (8.431.1)].

The PDF of Y is given by

$$f_Y(y) = \sum_{k=1}^{N} \sum_{i=1}^{m_{I_k}} \frac{\beta_k^{i-1} y^{m_{I_k}-1}}{(i-1)!} \exp\left(-\alpha_{I_k} y\right), \tag{9}$$

where β_k^{i-1} as defined before.

Upon substituting the CCDF of X_2 and the PDFs of X_1 and Y in (6), we get

$$F_X(x) = 1 - \underbrace{\frac{1 + K_1 \exp(-K_1)}{\eta_1} \sum_{k=0}^{N} \sum_{i=1}^{m_{I_k}} \frac{\beta_k^{i-1} \exp\left(-\frac{1+K_1}{\eta_1} x\right)}{(i-1)!}}_{C_1} \int_0^\infty Q\left(\sqrt{2K_2}, \sqrt{\frac{2(1+K_2)x(C+1)y}{\eta_2 z}}\right) \times I_0\left(2\sqrt{\frac{(1+K_1)K_1}{\eta_1}(z+x)}\right) \exp\left(-\frac{1+K_1}{\eta_1} z\right) y^{m_{I_k}-1} \exp\left(-\alpha_{I_k} y\right) dz dy. \tag{10}$$

Upon using the series representation of the Marcum Q-function in [20, Eq. (4.35)] and that of the Bessel function in [19, Eq. (8.447.1)], we get

$$F_X(x) = 1 - C_1 \exp(-K_2) \sum_{n=0}^{\infty} K_2^n \sum_{j=0}^{\infty} \frac{K_2^j \left(\frac{(1+K_2)x(C+1)}{\eta_2}\right)^j}{j!\,\Gamma(n+j+1)} \sum_{l=0}^{\infty} \frac{x^l}{(l!)^2} \left(\frac{(1+K_1)K_1}{\eta_1}\right)^l$$
$$\times \int_0^{\infty} y^{m_{I_k}+j-1} \exp(-\alpha_{I_k} y) \sum_{q=0}^{l} \binom{l}{q} x^{-q} \int_0^{\infty} z^{-j+q} \exp\left(-\frac{(1+K_2)x(C+1)y}{\eta_2 z} - \frac{1+K_1}{\eta_1} z\right) dz dy. \tag{11}$$

Now, with the help of [19, Eq. (3.471.9)] and [19, Eq. (6.643.3)], and after some algebraic manipulations, we get the result as in (4). □

For the special case where the interfering channels have the same fading parameter $\{m_{I_i}\}_{i=1}^N = m_I$ and experience the same average power $\{\Omega_{I_i}\}_{i=1}^N = \Omega_I$, the PDF of Y is given by

$$f_Y(y) = \frac{\alpha_I^{Nm_I}}{\Gamma(Nm_I)} y^{Nm_I-1} \exp(-\alpha_I y). \tag{12}$$

Upon substituting (12) in (6), and after following the same procedure as in Sect. 3, the outage probability for the i.i.d. case of this scenario can be evaluated as

$$P_{\text{out}}(\gamma_{\text{th}}) = 1 - \frac{\exp(-(K_1+K_2))}{\Gamma(Nm_I)} \exp\left(-\frac{1+K_1}{\eta_1}\gamma_{\text{th}}\right) \sum_{n=0}^{M_1} K_2^n \sum_{j=0}^{M_2} \frac{K_2^j\,\Gamma(j+Nm_I)}{j!\,\Gamma(n+j+1)} \Xi_3^{\frac{j}{2}}$$
$$\times \gamma_{\text{th}}^{\frac{j}{2}} \sum_{l=0}^{M_3} \frac{K_1^l}{(l!)^2} \left(\frac{1+K_1}{\eta_1}\right)^l \gamma_{\text{th}}^l \sum_{q=0}^{l} \binom{l}{q} \Xi_4^{\frac{q}{2}} \gamma_{\text{th}}^{\frac{-q}{2}} \Gamma(q+Nm_I+1) \exp\left(\frac{\Xi_3}{2}\gamma_{\text{th}}\right) W_{\hat{a},\hat{b}}(\Xi_3\gamma_{\text{th}}), \tag{13}$$

where $\Xi_3 = \Xi_1$ and $\Xi_4 = \Xi_2$ with replacing Ω_{I_k} by Ω_I, $\hat{a} = -\left(\frac{j}{2} + \frac{q}{2} + Nm_I\right)$, and $\hat{b} = \frac{-j+q+1}{2}$.

3.2 Symbol Error Probability

In this subsection, we derive the symbol error probability for the i.n.d. and i.i.d. cases of interferers' channels. The SEP is given by

$$\text{SEP} = \int_0^{\infty} a\,Q\left(\sqrt{2b\gamma}\right) f_{\gamma_D}(\gamma) d\gamma = \frac{a\sqrt{b}}{2\sqrt{\pi}} \int_0^{\infty} \frac{e^{-b\gamma}}{\gamma^{1/2}} F_{\gamma_D}(\gamma) d\gamma, \tag{14}$$

where $Q(\cdot)$ is the Gaussian Q-function, a and b are modulation specific constants.

Upon substituting the CDF $F_{\gamma_D}(\gamma) = P_{\text{out}}(\gamma)$ obtained in (4) in (14), and with the help of [19, Eq. (3.381.4)] and [19, Eq. (7.621.3)], and after some algebraic manipulations, the SEP for the i.n.d. case of this scenario can be evaluated as

$$\text{SEP} = \frac{a\sqrt{b}}{2\sqrt{\pi}} \Big\{ \Gamma\left(\frac{1}{2}\right) b^{-\frac{1}{2}} - \exp(-(K_1+K_2))\, \Xi_5^{-\frac{3}{2}} \Xi_1 \sum_{k=0}^{N} \Omega_{I_k}^{m_{I_k}} \sum_{i=1}^{m_{I_k}} \frac{\beta_k^{i-1}}{(i-1)!} \sum_{n=0}^{M_1} K_2^n \sum_{j=0}^{M_2} \frac{K_2^j}{j!}$$
$$\times \frac{\Gamma(j+m_{I_k})}{\Gamma(n+j+1)} \sum_{l=0}^{M_3} \frac{K_1^l\,\Gamma\left(l+\frac{3}{2}\right)\left(\frac{1+K_1}{\eta_1}\right)^l}{(l!)^2\,\Gamma\left(j+l+m_{I_k}+\frac{3}{2}\right)} \Xi_5^{-l} \sum_{q=0}^{l} \binom{l}{q} \Gamma(q$$

$$+m_{I_k}+1)\Gamma\left(-q+j+l+\frac{1}{2}\right)\left(\frac{\Omega_{I_k}(1+K_2)(C+1)}{\eta_2}\right)^q F\left(\hat{a},\hat{b};\hat{c};\frac{\Xi_5-\Xi_1}{\Xi_5}\right)\Big\}, \tag{15}$$

where $\Xi_5=\frac{1+K_1}{\eta_1}+b$, $F(.,.;.;.)$ is the Gauss hypergeometric function defined in [19, Eq. (9.100)], $\hat{a}=l+\frac{3}{2}$, $\hat{b}=q+m_{I_k}+1$, and $\hat{c}=j+l+m_{I_k}+\frac{3}{2}$.

For the special case where the interfering channels have the same fading parameter $\{m_{I_i}\}_{i=1}^N=m_I$ and experience the same average power $\{\Omega_{I_i}\}_{i=1}^N=\Omega_I$, upon substituting the CDF $F_{\gamma_D}(\gamma)=P_{\text{out}}(\gamma)$ obtained in (13) in (14), and with the help of [19, Eq. (3.381.4)] and [19, Eq. (7.621.3)], and after some algebraic manipulations, the SEP for the i.i.d. case of this scenario can be evaluated as

$$\begin{aligned}\text{SEP}=&\frac{a\sqrt{b}}{2\sqrt{\pi}}\Big\{\Gamma\left(\frac{1}{2}\right)b^{-\frac{1}{2}}-\frac{\exp\left(-(K_1+K_2)\right)}{\Gamma(Nm_I)}\Xi_5^{-\frac{3}{2}}\Xi_3\sum_{n=0}^{M_1}K_2^n\sum_{j=0}^{M_2}\frac{K_2^j}{j!}\frac{\Gamma(j+Nm_I)}{\Gamma(n+j+1)}\sum_{l=0}^{M_3}\frac{K_1^l}{(l!)^2}\\&\times\frac{\Gamma\left(l+\frac{3}{2}\right)}{\Gamma\left(j+l+Nm_I+\frac{3}{2}\right)}\Xi_5^{-l}\left(\frac{1+K_1}{\eta_1}\right)^l\sum_{q=0}^{l}\binom{l}{q}\Gamma(q+Nm_I+1)\Gamma\left(-q+j+l+\frac{1}{2}\right)\\&\times F\left(\hat{a},\hat{b};\hat{c};\frac{\Xi_5-\Xi_3}{\Xi_5}\right)\left(\frac{\Omega_I(1+K_2)(C+1)}{\eta_2}\right)^q\Big\},\end{aligned} \tag{16}$$

where $\hat{a}=l+\frac{3}{2}$, $\hat{b}=q+Nm_I+1$, and $\hat{c}=j+l+Nm_I+\frac{3}{2}$.

3.3 Asymptotic Analysis

Even thought the closed-form expressions of the outage probability and the SEP offer exact evaluation of the system performance, they are too complicated to give any insights about the system behavior. Therefore, in this subsection, we derive simple expressions for the outage probability and SEP at high SNR values where more information about the diversity order and coding gain of the system can be extracted. The asymptotic results will be for the Rayleigh/Nakagami-*m* fading environment which is a special case of the Rician/Nakagami-*m* fading scenario. In deriving the asymptotic expressions, finite number of interferers is assumed and finite powers. In other words, the interferers' powers are assumed to be not scaling with the SNR. For the Rician/Nakagami-*m* fading scenario, by letting $K_1=K_2=0$ in (13), we end up with the Rayleigh/Nakagami-*m* special case. The outage probability and SEP for the Rayleigh/Nakagami-*m* fading scenario at high SNR regime are summarized in the following Lemma.

Lemma 2 *The asymptotic outage probability and SEP for Rayleigh/Nakagami-m fading scenario can be respectively evaluated as*

$$P_{\text{out}}^{\infty}(\gamma_{\text{th}})=\gamma_{\text{th}}\left(\frac{1}{\eta_1}-\frac{Nm_I\Omega_I\sigma_{\text{sr}}^2}{\mu\eta_1}\left[\ln\left(\frac{\Omega_I\sigma_{\text{sr}}^2}{\mu\eta_1}\gamma_{\text{th}}\right)+\psi(Nm_I+1)+2c-1\right]\right), \tag{17}$$

$$\text{SEP}^{\infty}=\frac{a}{4b}\left\{\frac{1}{\eta_1}-\frac{Nm_I\Omega_I\sigma_{\text{sr}}^2}{\mu\eta_1}\left[\psi\left(\frac{3}{2}\right)-\ln\left(b\frac{\Omega_I\sigma_{\text{sr}}^2}{\mu\eta_1}\right)+\psi\left(Nm_I+1\right)+2c-1\right]\right\}. \tag{18}$$

Proof Upon letting $K_1 = K_2 = 0$ and taking only the first term of each summation as they are still dominant and using [21, Eq. (13.1.33)], the result in (13) can be rewritten in terms of the Tricomi hypergeometric function as

$$P_{\text{out}}(\gamma_{\text{th}}) = 1 - \Gamma(Nm_I + 1) \exp\left(-\frac{\gamma_{\text{th}}}{\eta_1}\right) \left(\frac{\Omega_I (C+1)}{\eta_1 \eta_2} \gamma_{\text{th}}\right) \Psi\left(Nm_I + 1, 2; \frac{\Omega_I (C+1)}{\eta_1 \eta_2} \gamma_{\text{th}}\right), \tag{19}$$

where $\Psi(.,;.)$ is the Tricomi hypergeometric function defined in [21, Eq. (13.1.6)].

Now, with the help of [21, Eq. (13.1.29)], the last result can be further simplified to

$$P_{\text{out}}(\gamma_{\text{th}}) = 1 - \Gamma(Nm_I + 1) \exp\left(-\frac{\gamma_{\text{th}}}{\eta_1}\right) \Psi\left(Nm_I, 0; \frac{\Omega_I (C+1)}{\eta_1 \eta_2} \gamma_{\text{th}}\right). \tag{20}$$

Upon letting $\eta_2 = \mu \eta_1$ and substituting the value of $(C + 1) \approx C$ in (20), we get

$$P_{\text{out}}(\gamma_{\text{th}}) = 1 - \Gamma(Nm_I + 1) \exp\left(-\frac{\gamma_{\text{th}}}{\eta_1}\right) \Psi\left(Nm_I, 0; \frac{\Omega_I \sigma_{\text{sr}}^2}{\mu \eta_1} \gamma_{\text{th}}\right). \tag{21}$$

As $\eta_1 \to \infty$, by using the Taylor expansion of the exponential function $\exp(-x) \approx \left(1 - \frac{x}{1!} + o\left(x^2\right)\right)$ and the asymptotic expression of the Tricomi function $\Psi(b, 0; x) \approx \frac{1}{\Gamma(b+1)} \left(1 + b\left[\ln x + \psi(b+1) + 2c - 1\right] x + o\left(x^2\right)\right)$, where $\psi(\cdot)$ is the digamma function and $c = 0.577215$ is the Euler-Mascheroni constant. By ignoring the high power terms $o\left(x^2\right)$ in these approximations and after some algebraic manipulations, the outage probability at high SNR values can be evaluated as in (17). Having the outage probability and hence, the CDF being derived, using (14), the SEP at high SNR values can be derived as in (18). □

4 Rician/Rician Environment

In this section, we evaluate the outage and symbol error probability performance of the Rician/Rician fading environment. Such fading scenario finds its applicability in micro-cellular mobile and indoor radio where a LOS propagation is existed between the base station and users in the desired cell.

4.1 Outage Probability

For this scenario, the channel coefficients of both the desired user h_{sr}, h_{rd} and the interferers' h_i are Rician distributed. Based on that, the channel gains $|h_{\text{sr}}|^2$, $|h_{\text{rd}}|^2$ are as defined in the first scenario and the gains $|h_i|^2$, $i = 1, \ldots, N$, are now i.i.d. non-central chi square distributed with parameters K_I and β_I. The outage probability for this scenario can evaluated as

$$\begin{aligned} P_{\text{out}}(\gamma_{\text{th}}) &= 1 - \exp\left(-\left(K_1 + K_2 + NK_I\right)\right) \exp\left(-\frac{1 + K_1}{\eta_1} \gamma_{\text{th}}\right) \\ &\times \sum_{n=0}^{M_1} K_2^n \sum_{j=0}^{M_2} \frac{K_2^j}{j!\,\Gamma(n+j+1)} \Xi_6^{\frac{j}{2}} \gamma_{\text{th}}^{\frac{j}{2}} \sum_{l=0}^{M_3} \frac{K_1^l}{(l!)^2} \left(\frac{1+K_1}{\eta_1}\right)^l \gamma_{\text{th}}^l \sum_{k=0}^{M_4} \frac{(NK_I)^k\, \Gamma(j+k+N)}{k!\,\Gamma(k+N)} \\ &\times \sum_{q=0}^{l} \binom{l}{q} \Gamma(k+q+N+1) \Xi_7^{\frac{q}{2}} \gamma_{\text{th}}^{\frac{-q}{2}} \exp\left(\frac{\Xi_6}{2} \gamma_{\text{th}}\right) W_{\tilde{a},\tilde{b}}\left(\Xi_6 \gamma_{\text{th}}\right), \end{aligned} \tag{22}$$

where $\Xi_6 = \Xi_3$ with replacing Ω_I by η_I, $\Xi_7 = \eta_1\eta_I(1+K_2)(C+1)/\eta_2(1+K_1)(1+K_I)$, $\bar{a} = -\left(\frac{j}{2}+k+\frac{q}{2}+N\right)$, and $\bar{b} = \frac{-j+q+1}{2}$.

In evaluating (22), the CDF of X_2 and the PDF of X_1 in γ_{D} are as given in Sect. 3. Assuming i.i.d. interferers channels, the PDF of Y is given by

$$f_Y(y) = \left(\frac{1+K_I}{\eta_I}\right)^{\frac{N+1}{2}} \exp\left(-\left(NK_I + \frac{1+K_I}{\eta_I}y\right)\right)\left(\frac{y}{NK_I}\right)^{\frac{N-1}{2}} I_{N-1}\left(2\sqrt{\frac{N(1+K_I)K_I}{\eta_I}y}\right), \tag{23}$$

where $\eta_I = \frac{1}{\beta_I}$ is the average power of the interferers and $I_{N-1}(\cdot)$ is the modified Bessel function of the second type and order $N-1$ defined in [19, Eq. (8.445)].

Upon substituting the CCDF of X_2, the PDF of X_1, and the PDF of Y in (6), and using the same procedure as in Sect. 3 with the help of [20, Eq. (4.35)], [19, Eq. (8.447.1)], and [19, Eq. (8.445)], and after some algebraic manipulations, the outage probability for this scenario can be evaluated as in (22).

4.2 Symbol Error Probability

Upon substituting the CDF $F_{\gamma_{\mathsf{D}}}(\gamma) = P_{\text{out}}(\gamma)$ obtained in (22) in (14), and with the help of [19, Eq. (3.381.4)] and [19, Eq. (7.621.3)], and after some algebraic manipulations, the SEP for this scenario can be evaluated as

$$\begin{aligned}\text{SEP} = \frac{a\sqrt{b}}{2\sqrt{\pi}}\Bigg\{&\Gamma\left(\frac{1}{2}\right)b^{-\frac{1}{2}} - \exp\left(-(K_1+K_2+NK_I)\right)\Xi_5^{-\frac{3}{2}}\Xi_6\sum_{n=0}^{M_1}K_2^n\sum_{j=0}^{M_2}\frac{K_2^j}{j!\,\Gamma(n+j+1)}\sum_{l=0}^{M_3}\frac{K_1^l}{(l!)^2}\\
&\times\Gamma\left(l+\frac{3}{2}\right)\Xi_5^{-l}\left(\frac{1+K_1}{\eta_1}\right)^l\sum_{k=0}^{M_4}\frac{\Gamma(j+k+N)}{k!\,\Gamma(k+N)\Gamma\left(j+l+k+N+\frac{3}{2}\right)}(NK_I)^k\sum_{q=0}^{l}\binom{l}{q}\\
&\times\Gamma\left(j+l-q+\frac{1}{2}\right)\Gamma(k+q+N+1)\left(\frac{\eta_I(1+K_2)(C+1)}{\eta_2}\right)^q F\left(\hat{a},\hat{b};\hat{c};\frac{\Xi_5-\Xi_6}{\Xi_5}\right)\Bigg\},\end{aligned} \tag{24}$$

where $\hat{a} = l+\frac{3}{2}$, $\hat{b} = k+q+N+1$, and $\hat{c} = j+l++k+N+\frac{3}{2}$.

4.3 Asymptotic Analysis

For the Rician/Rician fading scenario, by letting $K_1 = K_2 = K_I = 0$ in (22), we end up with the Rayleigh/Rayleigh special case. Following the same procedure as in Sect. 3, the asymptotic outage probability and SEP for this case can be respectively evaluated as

$$P_{\text{out}}^{\infty}(\gamma_{\text{th}}) = \gamma_{\text{th}}\left(\frac{1}{\eta_1} - \frac{N\eta_I\sigma_{\text{sr}}^2}{\mu\eta_1}\left[\ln\left(\frac{\eta_I\sigma_{\text{sr}}^2}{\mu\eta_1}\gamma_{\text{th}}\right) + \psi(N+1) + 2c - 1\right]\right), \tag{25}$$

$$\text{SEP}^{\infty} = \frac{a}{4b}\left\{\frac{1}{\eta_1} - \frac{N\eta_I\sigma_{\text{sr}}^2}{\mu\eta_1}\left[\psi\left(\frac{3}{2}\right) - \ln\left(b\frac{\eta_I\sigma_{\text{sr}}^2}{\mu\eta_1}\right) + \psi(N+1) + 2c - 1\right]\right\}. \tag{26}$$

5 Nakagami-*m*/Rician Environment

In this section, we evaluate the outage and symbol error probability performance of the Nakagami-*m*/Rician fading environment. Such fading scenario finds its applicability in micro-cellular mobile and indoor radio where a LOS propagation is existed between the base station and users in the desired cell.

5.1 Outage Probability

For this scenario, the channel coefficients of the desired user h_{sr}, h_{rd} are Nakagami-m distributed, while the interferers' channels coefficients h_i are Rician distributed. Based on that, the channel gains $|h_{\mathsf{sr}}|^2$, $|h_{\mathsf{rd}}|^2$ are now gamma distributed with parameters m_1 and $\frac{1}{\Omega_1}$, m_2 and $\frac{1}{\Omega_2}$, respectively, and the gains $|h_i|^2, i = 1, \ldots, N$, are as defined in the second scenario. The outage probability for this scenario can be evaluated as

$$P_{\text{out}}(\gamma_{\mathsf{th}}) = 1 - \frac{m_1^{m_1-1}}{\Omega_1^{m_1-1}\Gamma(m_1)} \exp\left(-NK_I\right) \gamma_{\mathsf{th}}^{m_1-1} \exp\left(\left(\frac{\Xi_8}{2} - \frac{m_1}{\Omega_1}\right)\gamma_{\mathsf{th}}\right) \sum_{j=0}^{m_2-1} \frac{\Xi_8^{\frac{j}{2}} \gamma_{\mathsf{th}}^{\frac{j}{2}}}{j!}$$
$$\times \sum_{k=0}^{m_1-1} \binom{m_1-1}{k} \gamma_{\mathsf{th}}^{-\frac{k}{2}} \Xi_8^{\frac{k}{2}} \sum_{i=0}^{M} \frac{\Gamma(k+i+N+1)}{i!\,\Gamma(i+N)} \Gamma(j+i+N)(NK_I)^i W_{\hat{a},\hat{b}}\left(\Xi_8\gamma_{\mathsf{th}}\right), \tag{27}$$

where $\Xi_8 = m_1 m_2 \eta_I (C+1)/\Omega_1\Omega_2(1+K_I)$, M is a parameter for series convergence and takes values from 1-50, $\hat{a} = -\left(\frac{j}{2} + \frac{k}{2} + i + N\right)$, and $\hat{b} = \frac{-j+k+1}{2}$.

In evaluating (27), the PDF of Y is as given by (23) and the CDF of X_2 and the PDF of X_1 are respectively given by

$$F_{X_2}(x) = 1 - \sum_{j=0}^{m_2-1} \frac{1}{j!} \left(\frac{m_2}{\Omega_2}\right)^j x^j \exp\left(-\frac{m_2}{\Omega_2}x\right), \tag{28}$$

$$f_{X_1}(x) = \frac{m_1^{m_1}}{\Omega_1^{m_1}\Gamma(m_1)} x^{m_1-1} \exp\left(-\frac{m_1}{\Omega_1}x\right), \tag{29}$$

where $F_{X_2}(x)$ is valid for integer values of m_2.

Upon substituting the CCDF of X_2, the PDF of X_1, and the PDF of Y in (6) and using the Binomial formula, we get

$$F_X(x) = 1 - \underbrace{\frac{m_1^{m_1}\left(\frac{1+K_I}{\eta_I}\right)^{\frac{N+1}{2}}}{\Omega_1^{m_1}\Gamma(m_1)} \left(\frac{1}{NK_I}\right)^{\frac{N-1}{2}} \exp\left(-NK_I\right) \exp\left(-\frac{m_1}{\Omega_1}x\right) \sum_{j=0}^{m_2-1} \frac{\left(\frac{m_2}{\Omega_2}\right)^j (x(C+1))^j}{j!}}_{C_2}$$
$$\times \int_0^\infty y^{j+\frac{N}{2}-\frac{1}{2}} \exp\left(-\frac{1+K_I}{\eta_I}y\right) I_{N-1}\left(2\sqrt{\frac{N(1+K_I)K_I}{\eta_I}y}\right) \sum_{k=0}^{m_1-1} \binom{m_1-1}{k} x^{-k+m_1-1}$$
$$\times \underbrace{\int_0^\infty z^{-j+k} \exp\left(-\frac{m_2 x(C+1)y}{\Omega_2 z} - \frac{m_1}{\Omega_1}z\right) dz\, dy}_{I_1}. \tag{30}$$

Upon evaluating I_1 with the help of [19, Eq. (3.471.9)], we get

$$F_X(x) = 1 - 2C_2 \sum_{k=0}^{m_1-1} \binom{m_1-1}{k} x^{-k+m_1-1} \left(\frac{m_2\Omega_1 x(C+1)}{m_1\Omega_2}\right)^{\frac{-j+k+1}{2}} \int_0^\infty y^{\frac{j+k+N}{2}} \exp\left(-\frac{1+K_I}{\eta_I}y\right)$$
$$\times I_{N-1}\left(2\sqrt{\frac{N(1+K_I)K_I}{\eta_I}y}\right) K_{-j+k+1}\left(2\sqrt{\frac{m_1 m_2 (C+1)x}{\Omega_1\Omega_2}y}\right) dy. \tag{31}$$

Unfortunately, a closed-form expression for the CDF in last result is very difficult, if not impossible, to be obtained. It can be evaluated in a series form by making the change of variables, $t^2 = y$, and using [19, Eq. (8.445)] and [19, Eq. (6.631.3)], and after some algebraic manipulations, the outage probability for this scenario can be evaluated as in (27).

5.2 Symbol Error Probability

Upon substituting the CDF $F_{\gamma_{\mathsf{D}}}(\gamma) = P_{\text{out}}(\gamma)$ obtained in (27) in (14), and with the help of [19, Eq. (3.381.4)] and [19, Eq. (7.621.3)], and after some algebraic manipulations, the SEP for this scenario can be evaluated as

$$\begin{aligned}\text{SEP} = \frac{a\sqrt{b}}{2\sqrt{\pi}}\Bigg\{&\Gamma\left(\frac{1}{2}\right)b^{-\frac{1}{2}} - \frac{m_1^{m_1}}{\Omega_1^{m_1}}\Xi_9^{-(m_1+\frac{1}{2})}\frac{\Gamma\left(m_1+\frac{1}{2}\right)}{\Gamma\left(m_1\right)}\Xi_{10}\exp\left(-NK_I\right)\sum_{j=0}^{m_2-1}\frac{1}{j!}\\ &\times\sum_{k=0}^{m_1-1}\binom{m_1-1}{k}\Gamma\left(j-k+m_1-\frac{1}{2}\right)\Xi_{10}^k\sum_{i=0}^{M}\frac{\Gamma(j+i+N)\Gamma(k+i+N+1)(NK_I)^i}{i!\,\Gamma(i+N)\Gamma\left(j+i+m_1+N+\frac{1}{2}\right)}\\ &\times F\left(\hat{a},\hat{b};\hat{c};\frac{\Xi_9-\frac{m_1}{\Omega_1}\Xi_{10}}{\Xi_9}\right)\Bigg\},\end{aligned} \tag{32}$$

where $\Xi_9 = \frac{m_1}{\Omega_1} + b$, $\Xi_{10} = m_2\eta_I(C+1)/\Omega_2(1+K_I)$ $\hat{a} = m_1 + \frac{1}{2}$, $\hat{b} = k+i+N+1$, and $\hat{c} = j+i+m_1+N+\frac{1}{2}$. It is worth to re-mention that the achieved results are valid for integer values of m_2.

5.3 Asymptotic Analysis

For the Nakagami-m/Rician fading scenario, by letting $m_1 = m_2 = 1$ in (27), we end up with the Rayleigh/Rician special case. Following the same procedure as in Sect. 3, the asymptotic outage probability and SEP for this case can be respectively evaluated as

$$P_{\text{out}}^{\infty}(\gamma_{\text{th}}) = \gamma_{\text{th}}\left(\frac{1}{\eta_1} - \frac{N\eta_I\sigma_{\text{sr}}^2}{\mu\eta_1(1+K_I)}\left[\ln\left(\frac{\eta_I\sigma_{\text{sr}}^2}{\mu\eta_1(1+K_I)}\gamma_{\text{th}}\right) + \psi(N+1) + 2c - 1\right]\right), \tag{33}$$

$$\text{SEP}^{\infty} = \frac{a}{4b}\left\{\frac{1}{\eta_1} - \frac{N\eta_I\sigma_{\text{sr}}^2}{\mu\eta_1(1+K_I)}\left[\psi\left(\frac{3}{2}\right) - \ln\left(b\frac{\eta_I\sigma_{\text{sr}}^2}{\mu\eta_1(1+K_I)}\right) + \psi\left(N+1\right) + 2c - 1\right]\right\}. \tag{34}$$

It is worth pointing out that the asymptotic expressions can be quantified in terms of diversity order and coding. The diversity order is defined as the negative slope of outage probability curves on a log-log scale, and the coding gain is defined as the shift of the curve in relative to the outage probability reference curve. At the high SNR regime, we can express the outage probability as $P_{\text{out}} \approx (G_{\mathsf{c}}\eta_1)^{-G_{\mathsf{d}}}$, where G_{d} is the achieved diversity order of the system and G_{c} is the coding gain. As we can see, for the case where the interferers' powers do not scale with the SNR, all the analyzed scenarios in this section have the same diversity order. Therefore, we can notice that for these special cases of fading scenarios that the degradation in system behavior comes through the coding gain. Noticing that the number of interferers affects the coding gain for all scenarios, in addition, to the effect of fading parameters m_I and K_I for Rayleigh/Nakagami-m and, Rayleigh/Rician, respectively.

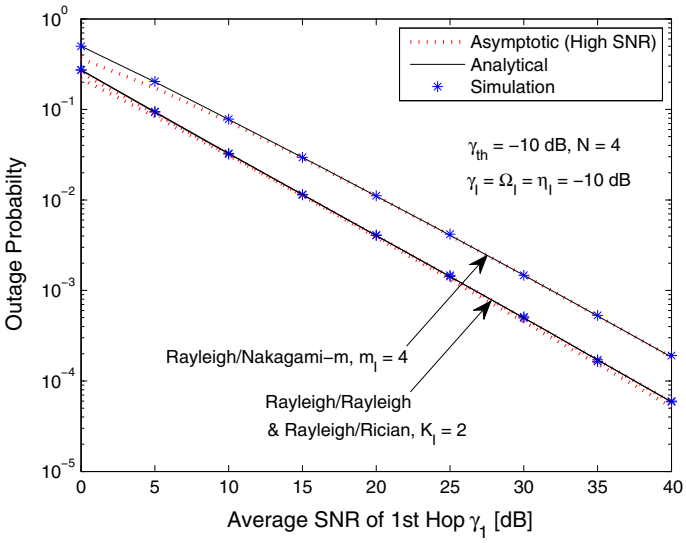

Fig. 1 Outage probability versus average SNR for fixed-gain AF relay system with CCI at destination for different fading environments

6 Numerical Results

In this section, we illustrate the validity of the expressions derived in Sects. 3, 4, and 5. We also discuss and compare the diversity order and the coding gain of some cases of the proposed fading environments. We also provide some numerical examples to illustrate the effect of interference and some system parameters as the fading parameters on the system performance.

Figure 1 illustrates the outage performance for some special cases of the proposed fading scenarios; Rayleigh/Rayleigh, Rayleigh/Nakagami-m, and Nakagami-m/Rayleigh cases. As can be seen, both the analytical and asymptotical results fit accurately with the simulation curves. A key result of our paper for the case where the interferers' channels possess Rician fading is that the Rician-K factor is hardly affecting the system performance which confirms the same result achieved in [18]. Also, for the case where the interferers' power do not scale with the SNR, we can notice that the different fading scenarios of the interferers' channels have the same diversity order. This can be inferred from the results of the asymptotic outage probability of all scenarios where the power of η_1^{-1} is the same. We can also notice that the interference degrades the system performance by only affecting the coding gain. Finally, it is clear to see that the coding gain of the Rayleigh/Nakagami-m, the Rayleigh/Rayleigh, and the Rayleigh/Rician fading scenarios is affected by the number, the fading parameters, and the average powers of the interferers.

Figures 2 and 3 validate the achieved analytical results. These two figures show that the considered Rician/Nakagami-m, Rician/Rician, and Nakagami-m/Rician fading scenarios simplify to the special case of Rayleigh/Rayleigh fading when their fading parameters are set to give this special case. The figures clearly illustrate that the three fading environments have the same performance under this condition. Also, the figures show that increasing the number of interferers increases the outage and error probabilities of the system, as expected.

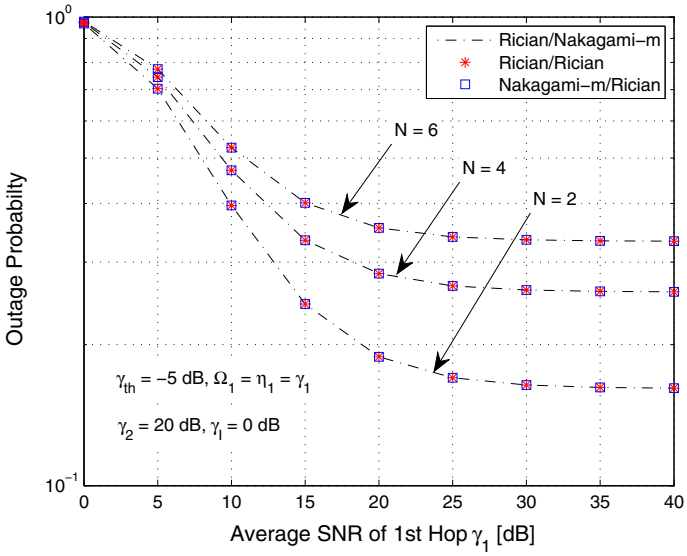

Fig. 2 Outage probability versus average SNR for fixed-gain AF relay system with CCI at destination for different fading environments when their fading parameters are set to give the special case of Rayleigh/Rayleigh fading

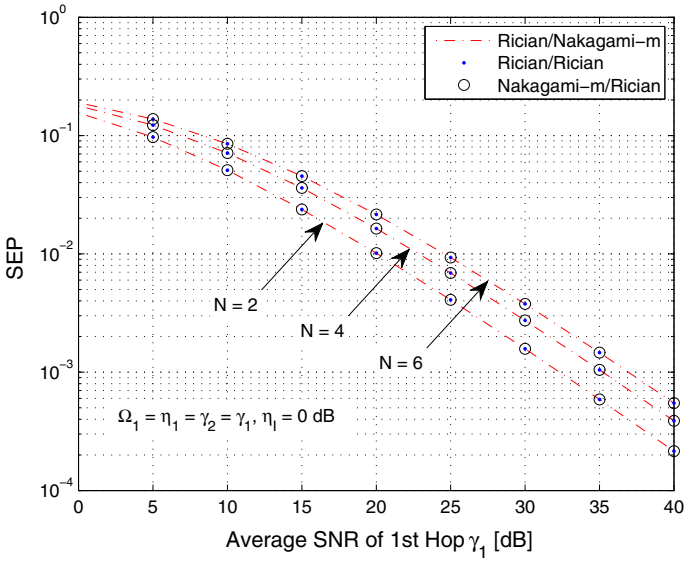

Fig. 3 Average SEP versus average SNR for fixed-gain AF relay system with CCI at destination for different fading environments when their fading parameters are set to give the special case of Rayleigh/Rayleigh fading

The outage performance of the Rician/Nakagami-*m* fading scenario is studied in Figs. 4, 5, and 6. Figure 4 is a validation to the achieved analytical results. We can notice from this figure the perfect fitting between the achieved expressions of this fading scenario and Monte-Carlo simulations. This is a strong indication on the accuracy of our derived analytical expressions.

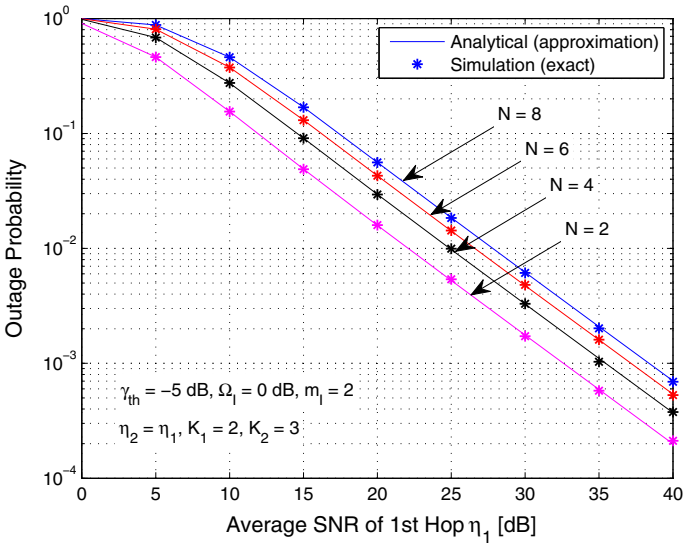

Fig. 4 Outage probability versus average SNR for fixed-gain AF relay system with CCI at destination for Rician/Nakagami-*m* fading scenario with different numbers of interferers *N*

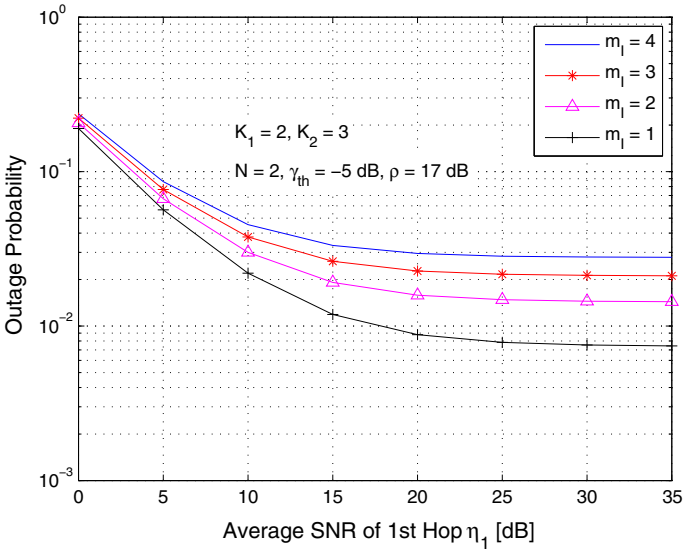

Fig. 5 Outage probability versus average SNR for fixed-gain AF relay system with CCI at destination for Rician/Nakagami-*m* fading scenario with different values of fading parameter m_I

In addition, this figure shows the degradation happens in system performance due to the increase in number of interferers *N*. Figure 5 studies the effect of the fading parameter of the interferers' channels m_I on the system behavior. As expected, as m_I increases and hence, the quality of the interferers' channels, the worse the achieved performance. Figure 6 illustrates the impact of the desired user channels via the power ratio ρ on the system behavior. This ratio represents the power of the second hop channel of the desired user to the power of

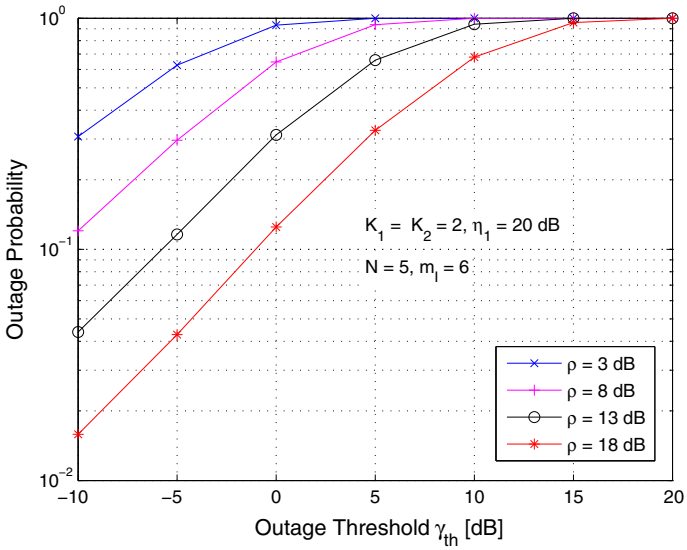

Fig. 6 Outage probability versus outage threshold for fixed-gain AF relay system with CCI at destination for Rician/Nakagami-*m* fading scenario with different values of power ratio ρ

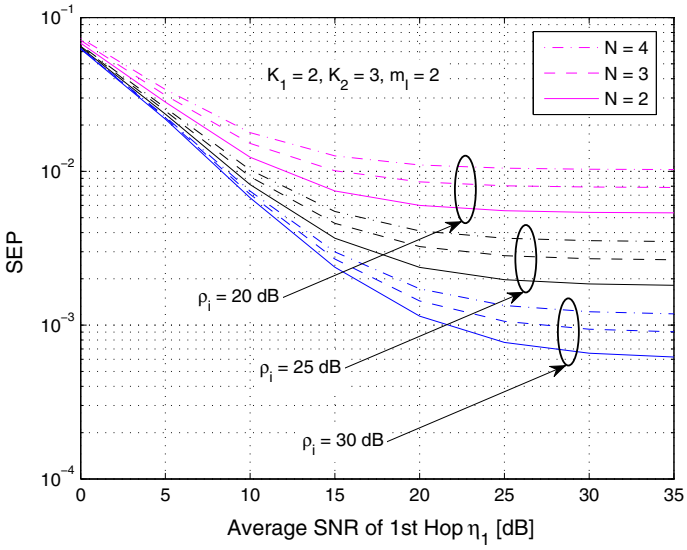

Fig. 7 Average SEP versus average SNR for fixed-gain AF relay system with CCI at destination for Rician/Nakagami-*m* fading scenario with different values of power ratio ρ_i and different numbers of interferers N

the interferers' channels $\eta_2/N\Omega_I$, where the interferers were assumed to be identical in this figure. As expected, as ρ increases, the system performance is more enhanced.

Figure 7 portrays the SEP performance of the Rician/Nakagami-*m* fading scenario for different values of power ratio ρ_i and different numbers of interferers N, where ρ_i denotes a ratio of the power of the second hop channel of the desired user to that of the channel of

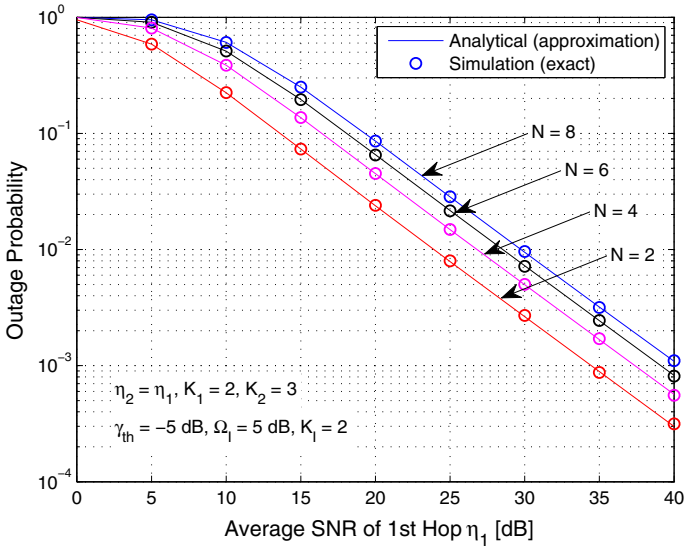

Fig. 8 Outage probability versus average SNR for fixed-gain AF relay system with CCI at destination for Rician/Rician fading scenario with different numbers of interferers

a single interferer η_2/Ω_I, where the interferers were assumed to be identical in this figure. As expected, as ρ_i increases, the better the achieved performance. Also, we can notice that the best behavior can be achieved when N takes its minimum value. Finally, a noise floor appears in all cases due to the effect of interference. Noticing that the diversity gain reaches zero as the interferers' powers were assumed to scale with the SNR in this figure.

The outage performance of the Rician/Rician fading scenario is studied in Figs. 8 and 9. Figure 8 illustrates the validity of the derived expressions. We can notice from this figure the perfect fitting between the achieved analytical results and Monte-Carlo simulations which is a strong indication on the accuracy of our derived expressions. In addition, the figure shows the degradation happens in system performance due to the increase in number of interferers N. Figure 9 studies the effect of the fading parameters K_1 and K_2 of the desired user channel on the system performance when they possess similar values. As can be seen, as the values of this pair increase and hence, the quality of the desired user channels, the better the achieved behavior.

The SEP performance of the Rician/Rician fading scenario is studied in Figs. 10 and 11. Figure 10 studies the effect of fading parameters K_1 and K_2 on the system performance when they possess different values. It is clear that the worst behavior is achieved when K_1 and K_2 equal unity. On the other hand, when they take the values (9,1), the achieved performance is better than the case of (1,9), specially, at low values of the first hop SNR. This means that the parameter K_1 is more effective when the average SNR of the first hop is smaller than that of the second hop. At the case when these SNRs are comparable, both cases are almost behaving the same. This is because the performance of the overall system is dominated by the interference affected worst link. Finally, the best behavior is achieved when K_1 and K_2 are equal and larger than unity. Figure 11 aims to show the inaccuracy in approximating the Rician fading model with the Nakagami-m model as an example. A big gap in system behavior can be seen in this figure when the the interferers' channels are approximated by Nakagami-m distribution instead of Rician distribution. In this figure, we used [20, Eq. (2.26)]

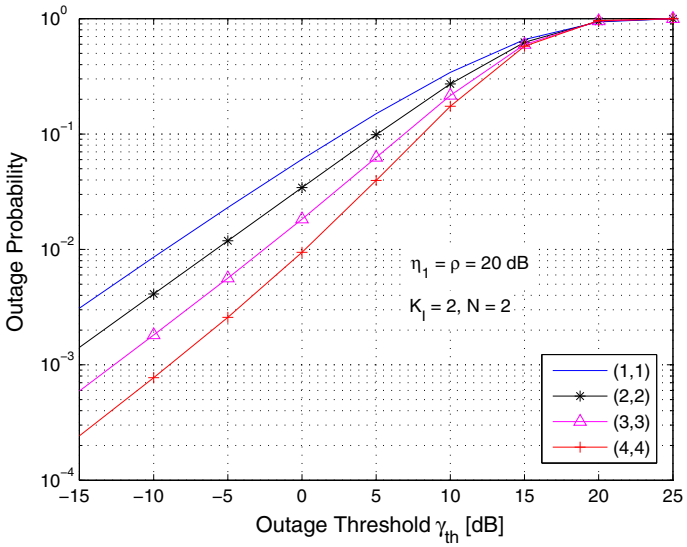

Fig. 9 Outage probability versus outage threshold for fixed-gain AF relay system with CCI at destination for Rician/Rician fading scenario with different values of fading parameters (K_1, K_2)

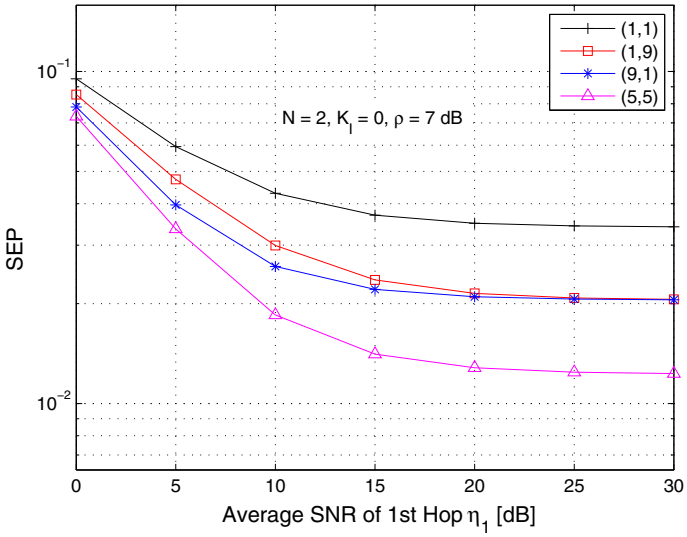

Fig. 10 Average SEP versus average SNR for fixed-gain AF relay system with CCI at destination for Rician/Rician fading scenario with different values of fading parameters (K_1, K_2)

to calculate the value of fading parameter m_I that approximates K_I. This result illustrates the importance of our assumption in modeling the interferers' channels to be Rician distributed and not to be approximated by any other fading models.

The outage performance of the Nakagami-m/Rician fading scenario is studied in Figs. 12 and 13. Figure 12 illustrates the validity of the derived expressions. A perfect fitting between the achieved analytical results and Monte-Carlo simulations can be seen in this figure. This

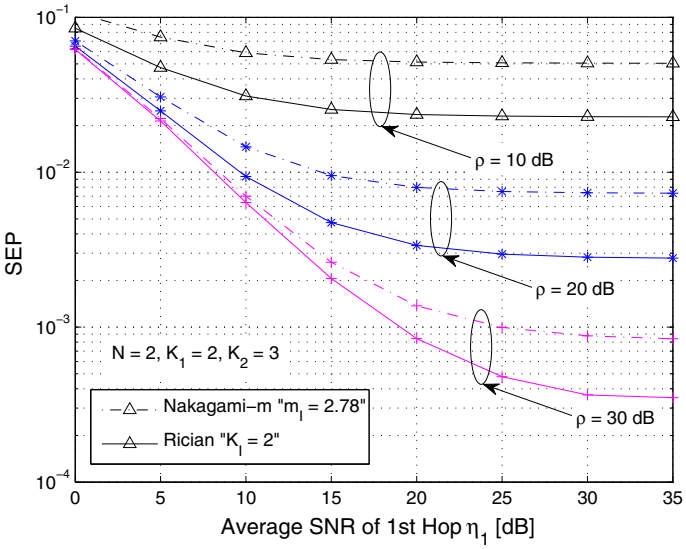

Fig. 11 Average SEP versus average SNR for fixed-gain AF relay system with CCI at destination for Rician/Rician and Rician/Nakagami-m fading scenarios with different values of power ratio ρ

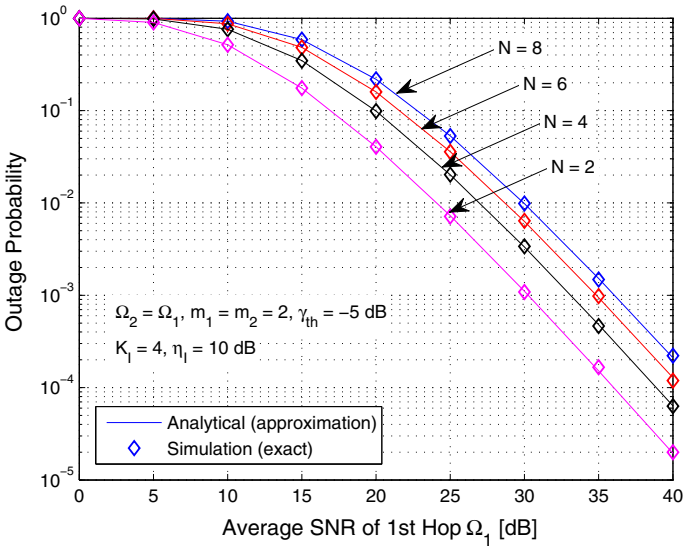

Fig. 12 Outage probability versus average SNR for fixed-gain AF relay system with CCI at destination for Nakagami-m/Rician fading scenario with different numbers of interferers N

is a clear evidence on the accuracy of our derived expressions. In addition, the figure shows the degradation happens in system performance due to the increase in number of interferers N. Figure 13 shows the impact of interferers' channels quality on the system behavior. As obvious, as η_I increases and hence, the quality of the interferers' signals, the worse the achieved behavior, as expected.

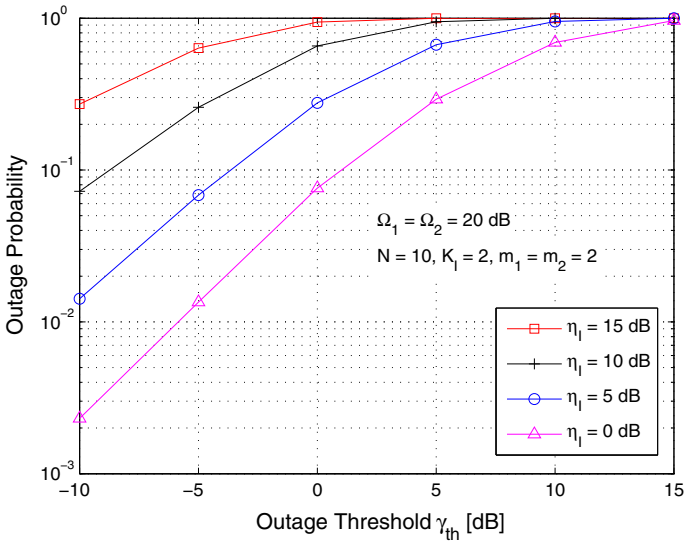

Fig. 13 Outage probability versus outage threshold for fixed-gain AF relay system with CCI at destination for Nakagami-*m*/Rician fading scenario with different values of interferers' power η_I

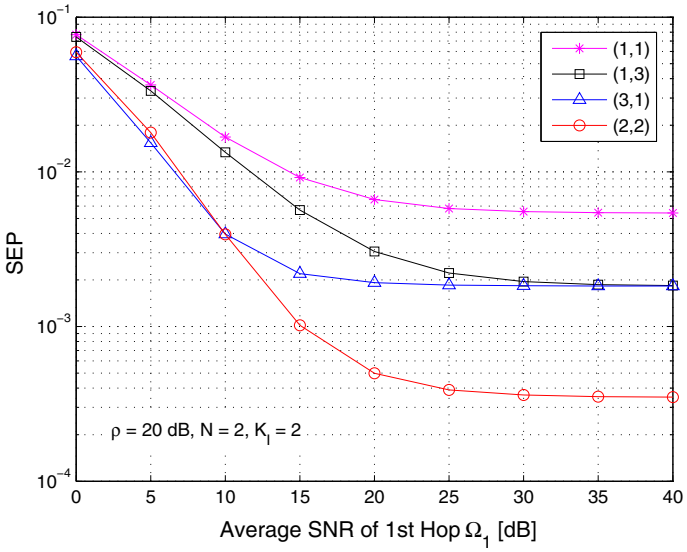

Fig. 14 Average SEP versus average SNR for fixed-gain AF relay system with CCI at destination for Nakagami-*m*/Rician fading scenario with different values of fading parameters (m_1, m_2)

Figure 14 studies the effect of fading parameters of the desired user channels m_1 and m_2 on the SEP performance of the Nakagami-*m*/Rician fading scenario. As explained in the case of Rician/Rician scenario and the effect of K_1 and K_2 on its performance, the same result can be seen here. The worst behavior is achieved when m_1 and m_2 equal unity which represents the Rayleigh fading. On the other hand, the case (3,1) gives better behavior than the case (1,3), specially, at low values of the first hop SNR. This means that the parameter m_1 is more

effective when the average SNR of the first hop is smaller than that of the second hop. At the case when these SNRs are comparable, both cases are almost behaving the same. This is because the performance of the overall system is dominated by the interference affected worst link. Finally, the best behavior is achieved when m_1 and m_2 are equal and larger than unity.

7 Conclusion

In this paper, we investigated the performance of a dual-hop fixed-gain AF relay system with co-channel interference at the destination. We considered various fading scenarios; Rician/Nakagami-*m*, Rician/Rician, and Nakagami-*m*/Rician. We derived accurate approximate expressions for the outage probability and the SEP for all the proposed fading models. Furthermore, we studied the system performance of the proposed scenarios at high SNR regime. We evaluated asymptotic expressions for the outage probability and the SEP in addition to evaluating the system diversity order and coding gain. The analytical and asymptotic results were validated by Monte-Carlo simulations. A perfect fitting between both the achieved analytical results and the asymptotic results with Monte-Carlo simulations was proved in some results. Also, for the case where the interferers' powers do not scale with the SNR, results showed that with different fading models for the interferers' channels, the interference is only affecting the system behavior through the coding gain without affecting the diversity order of the system. On the other hand, when the interferers' powers scale with the SNR, zero diversity gain is achieved for all fading scenarios. Other results illustrated the effect of number of interferers and the fading parameters on the system performance. Finally, results showed that approximating the Rician system model by the Nakagami-*m* one does not give accurate results at least in our presented study.

Acknowledgments This work is supported by King Fahd University of Petroleum & Minerals (KFUPM) through project of grant number FT121002. The paper was made possible by JSREP grant # 3-039-2-010 from the Qatar National Research Fund (a member of Qatar Foundation). The statements made herein are solely the responsibility of the authors.

References

1. Laneman, J. N., Tse, D. N. C., & Wornell, G. W. (2004). Cooperative diversity in wireless networks: Efficient protocals and outage behavior. *IEEE Transactions on Information Theory*, *50*(12), 3062–3080.
2. Mheidat, H., & Uysal, M. (2006). Impact of receive diversity on the performance of amplify-and-forward relaying under APS and IPS power constraints. *IEEE Communications Letters*, *10*, 468–470.
3. Senaratne, D. & Tellambura, C. (June 2009). Unified performance analysis of two hop amplify and forward relaying. In *Proceedings IEEE ICC*, Dresdn, Germany, pp. 1–5.
4. da Costa, D. B., Ding, H., & Ge, J. (May 2011). Interference-limited relaying transmissions in dual-hop cooperative networks over Nakagami-*m* fading. *IEEE Communications Letters, 15*(5), 503–505.
5. Al-Qahtani, F. S., Duong, T. Q., Zhong, C., Qaraqe, K. A., & Alnuweiri, H. (Aug 2011). Performance analysis of dual-hop AF systems with interference in Nakagami-*m* fading channels. *IEEE Signal Processing Letters, 18*(8), 454–457.
6. Milošević, N., Nikolić, Z. & Dimitrijević, B. (April 2011) Performance analysis of dual hop relay link in Nakagami-*m* fading channel with interference at relay. In *Proceedings 22nd International conference radioelektronika*, pp. 1–4.
7. Dohler, R., Lefranc, E., & Aghvami, H. (2003). Space-time block codes for virtual antenna arrays. In *Proceedings International conference on telecommunication*, France, pp. 198–203.
8. Zhong, C., Jin, S., & Wong, K. (2009). *Outage probability of dual-hop relay channels in the presence of interference* (pp. 1–5). *IEEE VTC Spring*.

9. Al-Qahtani, F., Zhong, C., Qaraqe, K., Alnuweiri, H., & Ratnarajah, T. (Dec 2011). Performance analysis of fixed-gain AF dual-hop relaying systems over Nakagami-m fading channels in the presence of interference. *EURASIP Journal on Wireless Communications and Networking*.
10. Hasna, M. & Alouini, M.-S. (Jan 2004). Harmonic mean and end-to-end performance of transmission systems with relays. *IEEE Transactions on Communications, 52*(1), 130–135.
11. Xu, W., Zhang, J., & Zhang, P., Outage probability of two-hop fixed-gain relay with interference at the relay and destination. *IEEE Communications Letters*, to be published.
12. da Costa, D. B. & Yacoub, M. D. (Sep. 2011). Outage performance of two hop AF relaying systems with co-channel interferers over Nakagami-*m* fading. *IEEE Communications Letters, 15*(9), 980–982.
13. Chen, S., Zhang, X., Liu, Fa. & Yang, D. (2010). Outage performance of dual-hop relay network with co-channel interference. In *Proceedings IEEE VTC Spring*, pp. 1–5.
14. Ikki, S. S., & Aïssa, S. (2010). Performance analysis of dual-hop relaying systems in the presence of co-channel interference. In *Proceedings IEEE GLOBECOM*, Miami, Florida.
15. Cvetković, A., Dordević, G., & Stefanović, M. (2011). Performance of interference-limited dual-hop non-regenerative relays over Rayleigh fading channels. *IET Communications*, *5*(2), 135–140.
16. da Costa, D. & Yacoub, M. (Aug 2011). Dual-hop DF relaying systems with multiple interferers and subject to arbitrary Nakagami-*m* fading. *Electronics Letttters*, pp. 999–1001.
17. Prasad, R., Kegel, A., & Loog, M. (1992). Cochannel interference probability for picocellular system with multiple Rician faded interferers. *Electronics Letters*, *28*(24), 2225–2226.
18. Suraweera, H. A., Michalopoulos, D. S., Schober, R., Karagiannidis, G. K. & Nallanathan, A. (June 2011). Fixed gain amplify-and-forward relaying with co-channel interference. In *Proceedings IEEE ICC*, Kyoto, Japan, pp. 1–6.
19. Gradshteyn, I. S., & Ryzhik, I. M. (2000). *Tables of integrals, series and products* (6th ed.). San Diago: Acadamic Press.
20. Simon, M. K., & Alouini, M.-S. (2005). *Digital communication over fading channels* (2nd ed.). London: Wiley.
21. Abramowitz, M., & Stegun, I. A. (1970). *Handbook of mathematical functions with formulas, graphs, and mathematical tables* (9th ed.). New York, NY: Dover Publications.

Anas M. Salhab Received the B.Sc. degree in Electrical Engineering from Palestine Polytechnic University (PPU), Hebron, Palestine, in 2004. He achieved his M.Sc. degree in Electrical Engineering from Jordan University of Science and Technology (JUST), Irbid, Jordan, in 2007. He received his Ph.D. degree from King Fahd University of Petroleum & Minerals (KFUPM), Dhahran, Saudi Arabia, in May 2013. He is currently a Postdoctoral Fellow in the Electrical Engineering Department at KFUPM. His research interest spans special topics in modeling and performance analysis of wireless communication systems, including cooperative relay networks, cognitive relay networks, and co-channel interference. Dr. Salhab served as a reviewer for IEEE TRANSACTIONS ON VEHICULAR TECHNOLOGY and IEEE COMMUNICATIONS LETTERS.

Fawaz S. Al-Qahtani Received the B.Sc. in electrical engineering from King Fahd University of Petroleum and Minerals (KFUPM), Saudi Arabia in 2000 and his M.Sc. in Digital Communication Systems from Monash University, Australia in 2005, and Ph.D. degree in Electrical and Computer Engineering, RMIT University, Australia. Since May 2010, he has been with Texas A&M University at Qatar, where he is an assistant research scientist. His research interests are digital communications, channel modeling, applied signal processing, MIMO communication systems, cooperative communications, cognitive radio systems, and physical layer security.

Salam A. Zummo Received the B.Sc. and M.Sc. degrees in Electrical Engineering from King Fahd University of Petroleum & Minerals (KFUPM), Dhahran, Saudi Arabia, in 1998 and 1999, respectively. He received his Ph.D. degree from the University of Michigan at Ann Arbor, USA, in June 2003. He is currently a Professor in the Electrical Engineering Department and the Dean of Graduate Studies at KFUPM. Dr. Zummo is a Senior Member of the IEEE. Dr. Zummo was awarded Saudi Ambassador Award for early Ph.D. completion in 2003, and the British Council/BAE Research Fellowship Awards in 2004 and 2006. He has more than 60 publications in international journals and conference proceedings in the area of wireless communications including error control coding, diversity techniques, MIMO systems, iterative receivers, multiuser diversity, multihop networks, user cooperation, interference modeling and networking issues for wireless communication systems.

Hussein Alnuweiri Received the master's degree from King Fahd University of Petroleum and Minerals, Dhahran, Saudi Arabia, in 1984, and the Ph.D. degree in electrical and computer engineering from the University of Southern California, Los Angeles, in 1989. He is currently a Professor and Program Chair of the Department of Electrical and Computer Engineering, Texas A&M University, Doha, Qatar. From 1991 to 2007, he was a Professor with the Department of Electrical and Computer Engineering University of British Columbia. From 1996 to 1998, he also represented the University of British Columbia, Vancouver, BC, Canada, at the ATM Forum. From 2000 to 2006, he served as a Canadian delegate to the ISO/IEC JTC1/SC29 Standards Committee (MPEG-4 Multimedia Delivery), where he worked within the MPEG-4 standardization JTC1-SC29WG11 and the Ad- Hoc group involved in the development of the reference software IM1 AHG. Dr. Alnuweiri has a long record of industrial collaborations with several major companies worldwide. He is also an inventor, and holds three U.S. patents and one international patent. He has authored or co-authored over 150 refereed journal and conference papers in various areas of computer and communications research. In particular, his research interests include mobile Internet technologies, multimedia communications, wireless protocols, routing and information dissemination algorithms for opportunistic networking, and quality-of-service provisioning and resource allocation in wireless networks.